

Physics-based Models for photonic thermometers

Zeeshan Ahmed^a

^a*National Institute of Standards and Technology, Physical Measurement Laboratory,
Sensor Science Division, 100 Bureau Drive, Gaithersburg, 20899, MD, USA*

Abstract

Resistance thermometry, meticulously developed over the last century, provides a time-tested method for taking temperature measurements. However, fundamental limits to resistance-based approaches along with a desire to reduce the cost of sensor ownership, increase sensor stability and meet the growing needs of emerging economy has produced considerable interest in developing photonic temperature sensors. In this study we utilize Della-Corte-Varshni treatment for thermo-optic coefficient to derive models for temperature-wavelength relationships in silicon ring resonators and Fiber Bragg gratings. Model evaluation is carried out using a Bayesian criteria that selects models for superior out-of-sample predictive accuracy whilst minimizing model complexity. Our work presents physics-based framework for photonic thermometry reference functions, putting constraints on model complexity and parameter bounds, pointing the way towards a reference function that can be utilized for future standardization and inter-comparison of photonic thermometers.

Keywords: Photonic thermometry, bandgap models, ring resonator, Fiber Bragg gratings, Bayesian model evaluation

PACS: 0000, 1111

2000 MSC: 0000, 1111

1. Introduction

The past two decades have witnessed tremendous advances in photonics leading to the development of novel photonic devices such as Bragg mirrors, ring resonators and photonic crystal cavities that are beginning to profoundly impact sensing [1, 2, 3]. Fiber Bragg Bragg gratings (FBG), for example, have been commercially available for decades and have found uses as sensors

in niche areas such as infrastructure monitoring and temperature sensing [4, 5, 6]. Photonic sensing differs from legacy-based resistance or voltage sensors in that the former relies on changes in material's refractive index (as opposed to charge transport) to transduce physical or chemical changes into frequency changes. In recent years, this dependence of photonic device's resonant wavelength on modal index has been exploited in a wide range of sensing applications ranging from temperature and pressure to chemical sensing in both the gas and liquid phase [2, 7, 8, 9]. Given the ability to measure frequency changes with very low uncertainties and economies of scale afforded by the telecom industry's use of 1550 nm light, photonic sensors have the potential to displace legacy sensors by providing superior or equivalent metrology performance while outperforming legacy infrastructure in the C-SWaP (Cost, Size, Weight and Power) metric [10, 2].

The potential impact of photonic sensors is most clearly visible in the field of temperature sensing. Photonic temperature sensors exploit the temperature dependent changes in a material's properties – namely, thermo-optic effect and thermal expansion to transduce temperature changes into frequency changes (see ref 2 and references within). For example, FBG exhibit temperature dependent shifts in resonance Bragg wavelength of ≈ 10 pm/K [5, 6, 4]. In dry, strain-free environments these can measure temperature with uncertainties of few hundred mK over 80 K to 1700 K [5, 6, 4]. On the other hand, silicon-on-insulator devices such as Bragg waveguides, ring resonators and photonic crystal cavities take advantage of silicon's superior thermo-optic coefficient (TOC) to deliver temperature sensitivities of 60 pm/K-80 pm/K [11, 12, 13, 14]. These devices have been demonstrated to measure temperature with sub-millikelvin resolution and are impervious to humidity [15, 16].

The photonic thermometry community has largely focused on sensor and instrumentation [2, 14, 13] development with detailed uncertainty quantification of the device taking a backseat. For baseline benchmarking, researchers have employed fitting to a linear function to estimate temperature-wavelength sensitivity metric [15, 14, 11]. While such an approach is useful in evaluating figures-of-merits e.g. sensitivity, limit of detection, linear range, *etc.* it does not lend itself to a physics-based interpretation of the data from a single device nor does it permit a physics-based explanation of variation in the response curve from device to device. As such this approach has limited utility when it comes to evaluating various measurement methodologies, devices across fabrication campaigns, and different laboratories. In this letter

we build on previous work in modeling of TOC to derive bandgap based models of Bragg gratings and ring resonators and evaluate these models against polynomials of degree 1 to 4.

2. Temperature-Wavelength Models

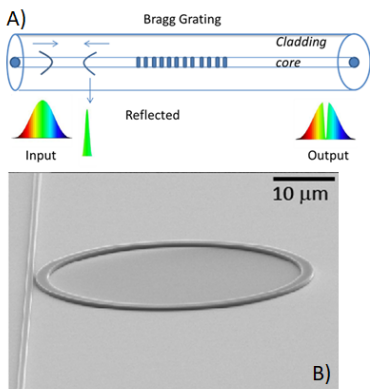


Figure 1: a) schematic of a Fiber Bragg grating and its working principle is shown. b) a scanning electron microscope image of a representative ring resonator is shown.

Modelling the TOC in semi-conductor and glasses has long been the subject of interest in the photonics community. Basic experimental and theoretical works have demonstrated the correlation between dielectric function of material and its band structure [17, 18, 19, 20, 21]. Della Corte *et. al.* [20] in their examination of TOC of silicon attributed the temperature dependence of refractive index to variations of the inter-band transition energies at critical points of silicon band structure. In this formulation, using the single oscillator approximation the refractive index is given as:

$$n^2 = 1 + \frac{E_p^2}{(E_g^2 - E^2)} \quad (1)$$

where E_p , E_g , and E are the electronic plasma energy, the average optical band gap energy and the photon energy, respectively. The thermo-optic coefficient is thus given by:

$$\frac{\partial n}{\partial T} = \frac{n^2 - 1}{2n} \left[-3\alpha_L - \frac{2}{E_g} \frac{\partial E_g}{\partial T} \frac{1}{1 - (\frac{E}{E_g})^2} \right] \quad (2)$$

where, α_L is the linear thermal expansion coefficient (LTE). The temperature dependence of energy bandgap is described by Varshni's empirical formula [19]

$$E_g(T) = E_g(0) - \frac{\alpha_g T^2}{T + \beta} \quad (3)$$

where $E_g(0)$ is the bandgap energy at 0 K, α_g is related to electron-phonon interaction and β is the Debye temperature. The authors demonstrated that for silicon a double oscillator model is necessary to capture its physics [20]. Here we use this methodology for modeling TOC to arrive at a temperature-wavelength model for FBG and ring resonators. For the case of FBG thermometer we note that the grating condition is given by $\lambda_B = 2n_{\text{eff}}\Lambda$, where λ_B is the Bragg wavelength, n_{eff} is the effective refractive index and Λ is the grating period. Taking a derivative of the grating equation with respect to temperature and substituting the TOC formulation above for a single oscillator approximation we arrive at:

$$\begin{aligned} \delta\lambda = & -c_1 \frac{T^3}{(T + \beta)^2} + c_2 \frac{T^2}{(T + \beta)^2} + c_3 \frac{T^2}{(T + \beta)} \\ & - T^R c_3 \frac{T}{(T + \beta)} + c_4 T + 2(n\alpha_L)T - c_5 T^R \end{aligned} \quad (4)$$

where, $\delta\lambda$ is wavelength detuning ($\lambda^T - \lambda^{T^R}$), $c_1 = 2\Lambda\alpha_g \frac{n^2-1}{2} \frac{1}{1-(\frac{E}{E_g})^2}$, $c_2 = 2\Lambda\alpha_L \frac{3(n^2-1)}{2n}$, $c_3 = 4\Lambda\alpha_g$, $c_4 = -2(3\Lambda\alpha_L \frac{n^2-1}{2n})$, $c_5 = 2n\alpha_L$, and T^R is the reference temperature (293.15K). Similarly for the case of silicon ring resonator, using a double oscillator model[20], we derive¹:

$$\begin{aligned} \delta\lambda = & -c_{11} \frac{T^3}{(T + \beta^{(1)})^2} - c_{22} \frac{T^3}{(T + \beta^{(2)})^2} + 2c_{11} \frac{T^2}{T + \beta^{(1)}} \\ & + c_{11} T^R \frac{T^2}{(T + \beta^{(1)})^2} + 2c_{22} \frac{T^2}{(T + \beta^{(2)})} + 2c_{22} T^R \frac{T^2}{(T + \beta^{(2)})^2} \\ & + 2c_{22} T^R \frac{T}{T + \beta^{(2)}} - 2c_{11} T^R \frac{T}{T + \beta^{(1)}} + 2\pi n_{\text{eff}} b_1 T^2 \\ & + (2\pi n_{\text{eff}} b_o - c_{11} - 2\pi n_{\text{eff}} b_1 T^R) T \\ & + (c_{11} T^R - 2\pi n_{\text{eff}} b_o T^R) \end{aligned} \quad (5)$$

¹we model thermal linear expansion using a first order linear model

Where, $c_{11} = 2\pi r \frac{2}{E_g} \frac{n^2-1}{2n} \frac{1}{1-(\frac{E}{E_g})^2} \alpha_g^{(1)}$ and $c_{22} = 2\pi r \frac{2}{E_g} \frac{n^2-1}{2n} \frac{1}{1-(\frac{E}{E_g})^2} \alpha_g^{(2)}$. Note that the superscripts on the Debye temperature and electron-phonon interaction terms denote the oscillator number (1 or 2) and the parameter r is the radius of the ring. When fitting either model the c_{ij} parameters are treated as composite variables. We note that the experimental temperature-wavelength data used here has previously been reported upon [22, 23].

We systematically evaluate the bandgap-based models against polynomial functions of order 1-4 by computing the leave-one-out cross validation score (LOO) and widely applicable information criteria (WAIC) scores [24] from the Markov Chain Monte Carlo trajectories of the fittings carried out in PyMC3 [25]. The LOO score provides a measure of model’s ability to generalize by estimating its out-of-sample error. In contrast the WAIC scores (waic score, standard error and effective number of parameters) in addition to evaluating for model’s predictive performance, penalize the model for complexity [24]. We use the LOO and WAIC scores to select for models that minimize out-of-sample uncertainty (testing error) while penalizing model complexity. As shown in Fig 1a, the LOO scores for a representative FBG sensor shows that polynomial functions ($n = 2, 3, 4$) outperform the bandgap-based model (eq. 4). Fixing the value of Debye temperature parameter fails to improve the predictive performance of the model. The difference in LOO score between the forth and third order polynomial ($\delta LOO = 0.35$) is statistically insignificant; the forth order polynomial model is further penalized for increased complexity (lower WAIC score) and therefore eliminated from further consideration. Over the entire dataset of 14 FBG sensors spanning the temperature range of 233 K to 393 K², the quadratic and cubic functions outperform the bandgap-based model for FBG. On average the training error for cubic functions (417 mK) is 21% lower than quadratic function (525 mK) indicating that over the temperature range examined, a cubic fit is an appropriate choice for modeling temperature-wavelength detuning behavior.

In the case of silicon ring resonator, over the limited temperature range examined here (298 K to 413 K), the bandgap-based model (eq 5) struggles to converge. The higher order terms containing the Debye temperature pa-

²original dataset contains two regenerate FBG sensors that span the temperature range of 373 K to 1073 K; these sensors were not considered in this study

rameters exhibit relatively flat likelihood profiles with MCMC trajectories exhibiting significant deviations past long burn-in times (50,000 to 100,000 steps) suggesting the bandgap model with its six free parameters is far too complex for an observed data that shows only weak deviation from linearity. If we simplify the model by assuming the $\beta \gg T$, the model takes on a quadratic form that easily converges. It is likely that the parameter space for the model in equation 5 contains degenerate solutions that force the MCMC trajectories in random walk between two (or more) basins resulting in unstable trajectories. As shown in Fig. 1d, the polynomial functions ($n = 2$ and 3) outperform other two models with cubic model holding a slight edge over quadratic function (average training error for cubic 2.6 mK vs 4 mK for quadratic function).

Even though the bandgap-based models under-performs for both FBG and silicon ring resonators, it does provide a useful framework to interpret the coefficients of polynomial models. The temperature sensitivity (first order term) contains contributions from only the linear thermo-optic coefficient and linear thermal expansion coefficient, whilst the higher order terms are sensitive to thermo-physical properties of the material (Debye temperature and electron-phonon interaction term) and shallow energy states that can be formed during the fabrication process and are susceptible to changes due to thermal cycling and strain engineering [26, 27]. Furthermore, the bandgap model indicates the cubic term carries a negative coefficient and in non-parameteric fitting it should not be constrained to positive values only. Together the cubic and quadratic terms serve to flatten the wavelength-temperature response at low temperatures. At high temperatures, the cubic term counteracts the quadratic term, serving to linearize the thermometer response at higher temperatures. The inflection point observed in the calibration data therefore can be interpreted as arising due to the effects of the higher order terms and as such is sensitive to material properties and fabrication processes that can introduce shallow states within the bandgap or alter the energies of pre-existing states. This would indicate researchers interested in engineering the response curve of photonic sensors should look beyond TOC and LTE and carefully examine the impact of material impurities and fabrication processes on the response curve. Fabrication processes may introduce significant variations in response curves from device to device, due to creation of shallow trap states or strain engineering, that unless accounted for, may impair attempts at achieving 100 mK-level inter-changeability.

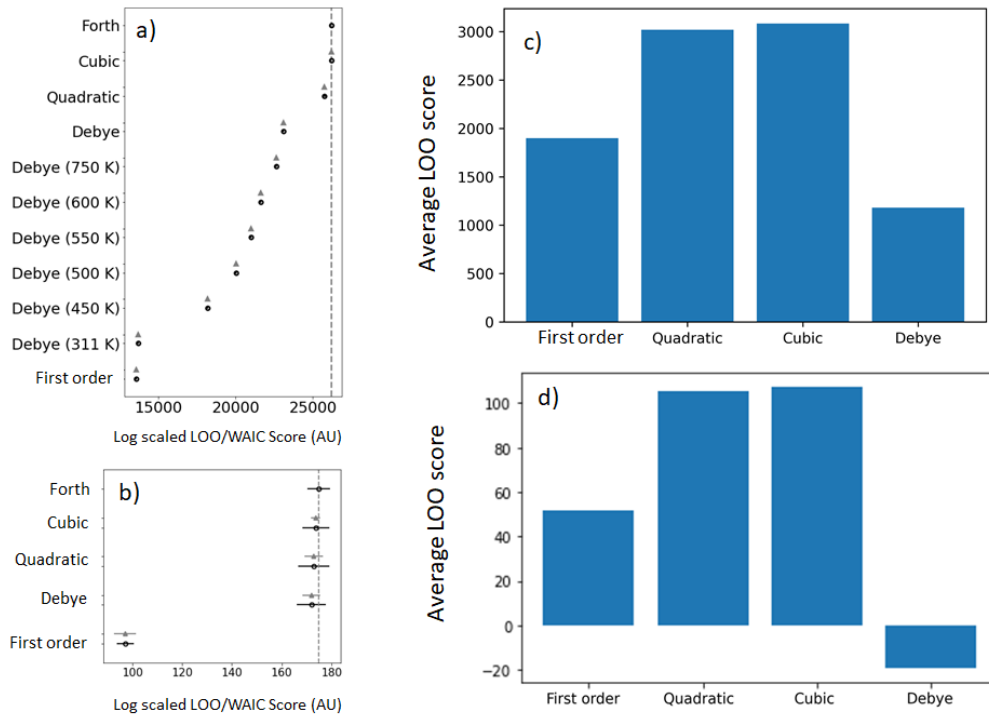


Figure 2: LOO scores for different model an individual FBG (a) and silicon ring resonator (b) are shown (dark circles; black error bars denote the standard deviation of LOO). For each model, the grey triangles present the difference of WAIC score between that model and the top model. Grey error bars indicates the standard error of the differences between the top-ranked WAIC and WAIC for each model. The mean LOO score for all models applied to FBG (c) and silicon ring resonator (d) sensor datasets show cubic functions outperform bandgap-based model.

3. Acknowledgments

Author wishes to acknowledge Gilad Kusne and Tyrus Berry for helpful conversations and Kartik Srinivasan for providing the SEM image of a ring resonator.

4. Disclosures

The author declares no conflicts of interest.

References

- [1] X. Wang, S. Grist, J. Flueckiger, N. A. F. Jaeger, L. Chrostowski, Silicon photonic slot waveguide bragg gratings and resonators, *Opt. Express* 21 (16) (2013) 19029–19039. doi:10.1364/OE.21.019029.
URL <http://opg.optica.org/oe/abstract.cfm?URI=oe-21-16-19029>
- [2] S. Dedyulin, Z. Ahmed, G. Machin, Emerging technologies in the field of thermometry, *Measurement Science and Technology* (2022).
URL <http://iopscience.iop.org/article/10.1088/1361-6501/ac75b1>
- [3] Q. Quan, M. Loncar, Deterministic design of wavelength scale, ultra-high q photonic crystal nanobeam cavities, *Opt. Express* 19 (19) (2011) 18529–18542. doi:10.1364/OE.19.018529.
URL <http://opg.optica.org/oe/abstract.cfm?URI=oe-19-19-18529>
- [4] R. Eisermann, S. Krenek, T. Habisreuther, P. Ederer, S. Simonsen, H. Mathisen, T. Elsmann, F. Edler, D. Schmid, A. Lorenz, A. A. F. Olsen, Metrological characterization of a high-temperature hybrid sensor using thermal radiation and calibrated sapphire fiber bragg grating for process monitoring in harsh environments, *Sensors* 22 (3) (2022). doi:10.3390/s22031034.
URL <https://www.mdpi.com/1424-8220/22/3/1034>
- [5] Z. Ahmed, J. Filla, W. Guthrie, J. Quintavalle, Fiber bragg grating based thermometry, *NCSLI Measure* 10 (4) (2015) 28–31. doi:10.1080/19315775.2015.11721744.
- [6] D. Grobnic, C. Hnatovsky, S. Dedyulin, R. B. Walker, H. Ding, S. J. Mihailov, Fiber bragg grating wavelength drift in long-term high temperature annealing, *Sensors* 21 (4) (2021). doi:10.3390/s21041454.
URL <https://www.mdpi.com/1424-8220/21/4/1454>
- [7] J. Scherschligt, J. A. Fedchak, Z. Ahmed, D. S. Barker, K. Douglass, S. Eckel, E. Hanson, J. Hendricks, N. Klimov, T. Purdy, J. Ricker, R. Singh, J. Stone, Review article: Quantum-based vacuum metrology at the national institute of standards and technology, *Journal of Vacuum Science & Technology A* 36 (4) (2018) 040801. arXiv:<https://doi.org/10.1116/1.5033568>, doi:10.1116/1.5033568.
URL <https://doi.org/10.1116/1.5033568>

- [8] M. R. Hartings, N. J. Castro, K. Gill, Z. Ahmed, A photonic ph sensor based on photothermal spectroscopy, *Sensors and Actuators B: Chemical* 301 (2019) 127076. doi:<https://doi.org/10.1016/j.snb.2019.127076>. URL <https://www.sciencedirect.com/science/article/pii/S0925400519312754>
- [9] T. Karrock, M. Gerken, Pressure sensor based on flexible photonic crystal membrane, *Biomed. Opt. Express* 6 (12) (2015) 4901–4911. doi:10.1364/BOE.6.004901. URL <http://opg.optica.org/boe/abstract.cfm?URI=boe-6-12-4901>
- [10] Z. Ahmed, N. Klimov, T. P. Purdy, T. Herman, K. Douglass, R. Fitzgerald, R. Kundagrami, Photonic thermometry: upending 100 year-old paradigm in temperature metrology, in: G. T. Reed, A. P. Knights (Eds.), *Silicon Photonics XIV*, Vol. 10923, International Society for Optics and Photonics, SPIE, 2019, pp. 56 – 63. doi:10.1117/12.2505898. URL <https://doi.org/10.1117/12.2505898>
- [11] N. N. Klimov, S. Mittal, M. Berger, Z. Ahmed, On-chip silicon waveguide bragg grating photonic temperature sensor, *Opt. Lett.* 40 (17) (2015) 3934–3936. doi:10.1364/OL.40.003934. URL <http://opg.optica.org/ol/abstract.cfm?URI=ol-40-17-3934>
- [12] N. Klimov, T. Purdy, Z. Ahmed, Towards replacing resistance thermometry with photonic thermometry, *Sensors and Actuators A: Physical* 269 (2018) 308–312. doi:<https://doi.org/10.1016/j.sna.2017.11.055>. URL <https://www.sciencedirect.com/science/article/pii/S0924424717318940>
- [13] C. Zhang, G. Kang, Y. Xiong, T. Xu, L. Gu, X. Gan, Y. Pan, J. Qu, Photonic thermometer with a sub-millikelvin resolution and broad temperature range by waveguide-microring fano resonance, *Opt. Express* 28 (9) (2020) 12599–12608. doi:10.1364/OE.390966. URL <http://opg.optica.org/oe/abstract.cfm?URI=oe-28-9-12599>
- [14] R. Eisermann, S. Krenek, G. Winzer, S. Rudtsch, Photonic contact thermometry using silicon ring resonators and tuneable laser-based spectroscopy, *tm - Technisches Messen* 88 (10) (2021) 640–654. doi:10.1515/teme-2021-0054. URL <https://doi.org/10.1515/teme-2021-0054>

- [15] H. Xu, M. Hafezi, J. Fan, J. M. Taylor, G. F. Strouse, Z. Ahmed, Ultra-sensitive chip-based photonic temperature sensor using ring resonator structures, *Opt. Express* 22 (3) (2014) 3098–3104. doi:10.1364/OE.22.003098.
URL <http://opg.optica.org/oe/abstract.cfm?URI=oe-22-3-3098>
- [16] J. A. Smith, P. Hill, C. Klitis, L. Weituschat, P. A. Postigo, M. Sorel, M. D. Dawson, M. J. Strain, High precision integrated photonic thermometry enabled by a transfer printed diamond resonator on gan waveguide chip, *Opt. Express* 29 (18) (2021) 29095–29106. doi:10.1364/OE.433607.
URL <http://opg.optica.org/oe/abstract.cfm?URI=oe-29-18-29095>
- [17] A. Arbabi, L. L. Goddard, Measurements of the refractive indices and thermo-optic coefficients of Si_3N_4 and SiO_2 using microring resonances, *Opt. Lett.* 38 (19) (2013) 3878–3881. doi:10.1364/OL.38.003878.
URL <http://opg.optica.org/ol/abstract.cfm?URI=ol-38-19-3878>
- [18] H. Gao, Y. Jiang, Y. Cui, L. Zhang, J. Jia, L. Jiang, Investigation on the thermo-optic coefficient of silica fiber within a wide temperature range, *Journal of Lightwave Technology* 36 (24) (2018) 5881–5886. doi:10.1109/JLT.2018.2875941.
- [19] Y. Varshni, Temperature dependence of the energy gap in semiconductors, *Physica* 34 (1) (1967) 149–154. doi:[https://doi.org/10.1016/0031-8914\(67\)90062-6](https://doi.org/10.1016/0031-8914(67)90062-6).
URL <https://www.sciencedirect.com/science/article/pii/0031891467900626>
- [20] F. G. Della Corte, M. Esposito Montefusco, L. Moretti, I. Rendina, G. Cocorullo, Temperature dependence analysis of the thermo-optic effect in silicon by single and double oscillator models, *Journal of Applied Physics* 88 (12) (2000) 7115–7119. arXiv:<https://doi.org/10.1063/1.1328062>, doi:10.1063/1.1328062.
URL <https://doi.org/10.1063/1.1328062>
- [21] G. E. Jellison, F. A. Modine, Optical functions of silicon between 1.7 and 4.7 eV at elevated temperatures, *Phys. Rev. B* 27 (1983) 7466–7472. doi:10.1103/PhysRevB.27.7466.
URL <https://link.aps.org/doi/10.1103/PhysRevB.27.7466>

- [22] N. Klimov, Z. Ahmed, Ring resonator thermometry, in: 2016 IEEE Photonics Conference (IPC), 2016, pp. 99–100. doi:10.1109/IPCon.2016.7830998.
- [23] Z. Ahmed, Hysteresis compensation in temperature response of fiber bragg grating thermometers using dynamic regression, *Sensors and Actuators A: Physical* 347 (1) (2022) 113872. doi:<https://doi.org/10.1016/j.sna.2022.113872>.
- [24] A. Vehtari, A. Gelman, J. Gabry, Practical bayesian model evaluation using leave-one-out cross-validation and waic, *Statistics and computing* 27 (5) (2017) 1413–1432.
- [25] J. Salvatier, T. V. Wiecki, C. Fonnesbeck, Probabilistic programming in python using pymc3, *PeerJ Computer Science* 2 (2016) e55.
- [26] T. Erdogan, V. Mizrahi, P. J. Lemaire, D. Monroe, Decay of ultraviolet-induced fiber bragg gratings, *Journal of Applied Physics* 76 (1) (1994) 73–80. arXiv:<https://doi.org/10.1063/1.357062>, doi:10.1063/1.357062. URL <https://doi.org/10.1063/1.357062>
- [27] H. Patrick, S. L. Gilbert, A. Lidgard, M. D. Gallagher, Annealing of bragg gratings in hydrogen-loaded optical fiber, *Journal of Applied Physics* 78 (5) (1995) 2940–2945. arXiv:<https://doi.org/10.1063/1.360753>, doi:10.1063/1.360753. URL <https://doi.org/10.1063/1.360753>